Endonuclease G: A role for the enzyme in recombination and cellular proliferation

Ke-Jung Huang*, Chia-Chi Ku†, and I. Robert Lehman*‡

Departments of *Biochemistry and †Pediatrics, Stanford University School of Medicine, Stanford, CA 94305

Contributed by I. Robert Lehman, April 27, 2006

Our earlier studies had suggested that endonuclease G (EndoG), a member of the evolutionarily conserved DNA/RNA nonspecific $\beta\beta\alpha$-Me-finger nuclease family, functioned in the *a* sequence-mediated segment inversion observed during herpes simplex virus 1 replication. To test this hypothesis, we used RNA interference to reduce the level of EndoG in mammalian cells in culture. Reduction of EndoG produced a small but statistically significant decrease in *a* sequence-mediated recombination, suggesting that EndoG does play a role in this process. We also observed that reduction in the level of EndoG resulted in a deficiency in cell proliferation. Cells with a reduced level of EndoG also showed changes in cell distribution in the cell cycle, producing a pattern characteristic of cells that have been arrested in the G_2 phase. These findings suggest that EndoG is required for normal cellular proliferation.

herpes simplex virus 1 | short hairpin RNA | cell cycle | nuclease | HSV-1 *a* sequence

Endonuclease G (EndoG) belongs to a group of conserved, DNA/RNA nonspecific $\beta\beta\alpha$-metal-ion-finger nucleases (1). In the mouse, EndoG is expressed in the cytoplasm as a precursor of ≈33 kDa, which is converted into the mature form of ≈28 kDa when it enters the mitochondria (2). EndoG is capable of digesting double- and single-stranded DNA and DNA·RNA heteroduplexes (2–5). With double-stranded DNA as substrate, EndoG first generates single-stranded breaks preferentially in $(dG)_n{\cdot}(dC)_n$ homopolymer sequences followed by double-stranded breaks (3, 6, 7). EndoG also generates double-stranded breaks in R loops (7) and cleaves DNA with cisplatin-mediated damage (8). Although EndoG is present predominantly in the intermembrane space of mitochondria (7, 9, 10), it is also found in the nucleus (2, 11). It has been suggested that EndoG functions in mitochondrial DNA synthesis (2) and apoptosis (10, 12). However, its role in those cellular functions remains controversial, as does its requirement for cell viability (9).

Our interest in EndoG originated in our studies of the genomic inversion that occurs during herpes simplex virus 1 (HSV-1) DNA replication. The HSV-1 genome consists of a linear 152-kb double-stranded DNA comprising two unique segments, L and S (13). The HSV-1 *a* sequence, a recombinogenic sequence containing 83% G+C (14, 15), is present as a direct repeat at the two termini of the viral genome and as an inverted repeat at the junction of L and S. Breakage at the HSV-1 *a* sequence is believed to trigger a recombination reaction resulting in inversion of the L and the S segments, producing the four possible isomers (16–18). In a previous study, we purified EndoG from HeLa cell nuclei and demonstrated that under our experimental conditions, EndoG is the only cellular enzyme capable of generating double-stranded breaks at the HSV-1 *a* sequence (6). We therefore hypothesized that EndoG initiates the recombinational event that triggers HSV-1 segment inversion. In this study, we tested this hypothesis by using RNA interference to reduce the cellular level of EndoG, and we found that EndoG very likely participates in this process. In the course of these studies, we observed that reduction in the level of EndoG resulted in a cell-proliferation defect.

Results

Specific Knockdown of EndoG. Plasmids pS and pS-RT were used as backbone plasmids to construct plasmids that produce EndoG knockdown. As shown in Fig. 1, three segments of 19 nucleotides in the EndoG gene were used as targets. Plasmids constructed according to these sequences were pT1, pT3, and pT5m (pS-based plasmids) and pT1-RT, pT3-RT, and pT5m-RT (pS-RT-based plasmids). In addition to producing short hairpin RNA (shRNA) from the U6 promoter to knock down EndoG, these plasmids provided antibiotic-resistance genes (G418 resistance for pS-derived plasmids, and puromycin resistance for pS-RT-derived plasmids) that permitted the elimination of untransfected cells.

To determine the extent of the reduction of EndoG expression, each of the plasmids was delivered into Vero cells. The cells were grown in G418-containing medium for 5 days, and the EndoG mRNA level was examined by RT-PCR. As shown in Fig. 2*A* and summarized in Fig. 2*B*, pT5m produced a 84% decrease in EndoG mRNA relative to the EndoG mRNA of cells containing pS, the control plasmid. Plasmid pT1 resulted in a 24% decrease, and pT3 resulted in a 44% decrease in the level of EndoG mRNA.

Reduction of EndoG Results in a Reduction in *a* Sequence-Mediated Recombination. To determine whether the reduction of EndoG influenced the recombination mediated by the HSV-1 *a* sequence, we used a model system based on plasmid pRD105, which carries an HSV-1 replication origin (*ori*S) and two direct repeats of the HSV-1 *a* sequence flanking 4.3-kb and 3-kb segments. Recombination between the two *a* sequences will remove the fragment between them. We first introduced pS, pT1, and pT5m into Vero cells and grew them for 5 days in medium containing G418. pRD105, which was packaged into a defective HSV-1 particle as a concatemer, was delivered into the Vero cells followed by infection with HSV-1. The recombination products were detected by Southern blotting. Cells lacking pS, pT1, or pT5m were either eliminated (>99%) or could not support HSV-1 replication because of their sensitivity to G418 (data not shown).

Fig. 3*A* illustrates the concatemeric pRD105, the predicted recombination products (R1 and R2), and the monomeric pRD105 (P). Fig. 3*B* shows the result of a typical recombination reaction. After 6 h of infection, the 7.3-kb pRD105 (P) and the recombination products R1 (11.3 kb) and R2 (3 kb) are visible. When infection proceeded to 12 h, synthesis of pRD105 increased substantially, as did the recombination products. This system therefore displayed an association between *a* sequence-mediated recombination and replication of pRD105, consistent with the association of HSV-1 genomic inversion and replication. Fig. 3*C* summarizes the results from five individual experiments.

Conflict of interest statement: No conflicts declared.

Abbreviations: EndoG, endonuclease G; hPBGD, human porphobilinogen deaminase; HSV-1, herpes simplex virus 1; PI, propidium iodide; shRNA, short hairpin RNA.

‡To whom correspondence should be addressed. E-mail: blehman@cmgm.stanford.edu.

BIOCHEMISTRY

```
   1 GGCACGAGGC TGGGTTCCGA GGCCCAAGCC CTTGGCAGTG
  41 TTTGTGAGTG GAAGGGAGGT CACGCTATCG TCCGCGGCCC
  81 CAGCAGCCCT GTGCCCTCGT TGGATCCCGC GACGCGGCTC
 121 CTTTAAGAGC CTCGCGGGTC GCCCGCCGCT AGGTCGCTCC
 161 CCGGCCATGC GGGCGCTGCG GGCCGGCCTG ACCCTGGCGT
 201 CGGGCGCGGG GCTGGGTGCG GTCGTCGAGG GCTGGCGGCG
 241 GCGGCGGGAG GACGCGCGGG CGGCGCTGGG ACTGCTGGGC
 281 CGGCTGCCCG TGCTGCCCGT GGCGGCGGCA GCCGAGTTGC
 321 CCCCTGTGCC CGGGGGACCC CGCGGCCCGG GCGAGTTGGC
 361 CAAGTACGGG CTGCCGGGGC TGGCGCAGCT CAAGAGCCGC
 401 GAGTCGTACG TGCTGTGCTA CGACCCGCGC ACCCGCGGCG
 441 CGCTCTGGGT GGTGGAGCAG CTGCGACCCG AGCGTCTCCG
 481 CGGCGACGGC GACCGGCGCG AGTGCGACTT CCGCGAGGAC
 521 GACTCGGTGC ACGCGTACCA CCGTGCCACC AACGCCGACT
 561 ACCGCGGCAG TGGCTTCGAC CGCGGTCACC TGGCCGCCGC
 601 CGCCAACCAC CGCTGGAGCC AGAAGGCCAT GGACGACACG
 641 TTCTACCTGA GCAAAGTCGC GCCCCAGGTG CCCCACCTCA
 681 ACCAGAATGC CTGGAACAAC CTGGAGAAAT ATAGCCGCAG
 721 CTTGACCCGC AGCTACCAAA ACGTCTATGT CTGCACAGGG
 761 CCACTCTTCC TGCCCAGGAC AGAGGCTGAT GGGAAATCCT
 801 ACGTAAAGTA CCAGGTCATC GGCAAGAACC ACGTGGCAGT
 841 GCCCACACAC TTCTTCAAGG TGCTGATCCT GGAGGCAGCA
 881 GGTGGGCAAA TTGAGCTCCG CACCTACGTG ATGCCCAACG
 921 CACCTGTGGA TGAGGCCATC CCACTGGAGC GCTTCCTGGT
 961 GCCCATCGAG AGCATTGAGC GGGCTTCGGG GCTGCTCTTT
1001 GTGCCAAACA TCCTGGCGCG GGCAGGCAGC CTCAAGGCCA
1041 TCACGGCGGG CAGTAAGTGA GGGTGGAGCC CAGTGAGACT
1081 GTGGGTGTGT GCAGGCCGGG GAGTATTAAA GGTGGTGATT
1121 TTTGGAAAAA AAA
```

Fig. 1. Human EndoG nucleotide sequences and the three 19-mers selected as shRNA targets. Nucleotide sequences (underlined) at positions 28–46 (T1), 682–700 (T3), and 693–711 with an A-to-T mutation at 708 (T5m) were selected to construct pT3, pT1, and pT5m with pS as the plasmid backbone. The translation start site (bold ATG) is at 167–169. T3 and T5m overlap by 8 nucleotides (dashed line). These sequences were also used to construct pT1-RT, pT3-RT, and pT5m-RT, with pS-RT as the plasmid backbone.

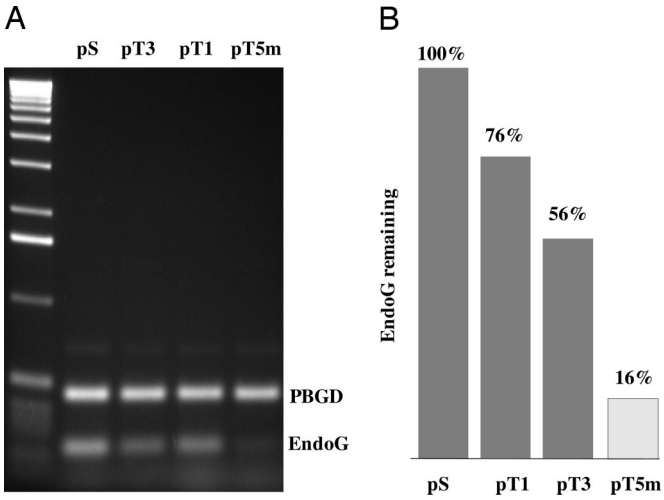

Fig. 2. Reduction of EndoG by RNA interference. (*A*) Agarose gel electrophoresis showing RT-PCR products obtained from cells transfected for 5 days with pS, pT1, pT3, and pT5m in the presence of G418. The positions of the 241-bp fragment representing EndoG and the 465-bp fragment representing the internal control human porphobilinogen deaminase (hPBGD) are indicated. (*B*) Intensity of the EndoG band of each sample, measured and normalized to that of the hPBGD band. The normalized EndoG value of each sample was compared with that of the cells containing pS.

The efficiency of recombination decreased in the following order: pS > pT1 > pT5m. This trend was detected at both 6 h and 12 h after coinfection with defective particles containing pRD105 and HSV-1. When examined by the *t* test, as summarized in Fig. 3*D*, the difference between almost any pair of transfected cells was statistically significant (≤ 0.03). The only exception was the difference between pT1- and pS-transfected cells at 12 h after infection. In that case, the value of the recombination products varied over a wide range. Therefore, the decrease in recombination efficiency, although small, is directly related to the decrease in EndoG level, suggesting that EndoG is involved in HSV-1 *a* sequence-mediated recombination.

Decrease in Viability of Cells with Reduced EndoG. In the course of these studies, we noted that the number of live cells containing pS, pT1, pT3, and pT5m differed significantly after 5 days of incubation in medium containing G418. As shown in Fig. 4, cells containing pS showed a 2.7-fold increase in live cells, whereas pT1, pT3, and pT5m showed a 2.4-, 1.5-, and 1.2-fold increase, respectively. Untransfected cells were essentially undetectable. As shown in Figs. 2*B* and 4, the greater the reduction of EndoG, the greater the proliferation defect. The same effect was observed when similar experiments were performed with 293T cells in the absence of antibiotic (data not shown). Experiments with pS-RT-derived plasmids (pS-RT, T1-RT, T3-RT, and T5m-RT) with 293T cells in the presence of puromycin showed a similar effect (data not shown).

We next determined whether the cell-proliferation defect could be rescued by exogenous expression of EndoG. Exogenous expression of EndoG is known to cause cell death (1). In an effort to reduce cell death, different EndoG fusions were tested. EndoG with its carboxyl terminus fused to the green fluorescent protein, EndoG-GFP, showed a reduced toxicity (data not shown). We therefore transfected pEndoG-GFP into 293T cells with pS-RT (a counterpart of pS) or pT5m-RT (a counterpart of pT5m). Twenty-four hours after transfection, the cells were treated with trypsin and seeded onto plates at ≈25% of the original cell density. The number of live cells was counted after growing cells in puromycin-containing medium for another 2 days, which is sufficient to eliminate untransfected cells.

As summarized in Fig. 5*A*, bar 3, when pT5m-RT was transfected into the cells with an empty vector pRK5, the cell number decreased to 73% relative to the control cells (cells cotransfected with pS-RT and pRK5; bar 1). Although this decrease in cell number is lower than that seen in Fig. 4 (44% decrease), because of a shorter incubation time (3 vs. 5 days), it demonstrates that the cell-proliferation defect originated from pT5m-RT. When pT5m-RT was transfected into the cells with pEndoG-GFP (bar 4), the cell number increased to 84% relative to the control cells (bar 1). The increase in live cells was dosage-dependent. As shown in Fig. 5*B*, bar 4, when twice the amount (400 ng vs. 800 ng) of pEndoG-GFP and pT5m-RT was transfected, the cell number increased to approximately the same level (103%) as the control cells. In contrast, expression of EndoG-GFP in cells containing the control plasmid pS-RT caused substantial cell death (50% live cells in Fig. 5*A*, bar 2, and 9% live cells in Fig. 5*B*, bar 2). Thus, exogenous expression of EndoG-GFP rescued the cell-proliferation defect, and the cell-proliferation defect resulted specifically from the reduction of EndoG. Moreover, reduction of EndoG by pT5m-RT also reversed the cell toxicity resulting from exogenous expression of EndoG-GFP, a demonstration that pT5m-RT reduces total EndoG activity in addition to reducing its mRNA level.

EndoG Deficiency Changes Cell Distribution in the Cell Cycle. To investigate further the cell-proliferation defect produced by the reduction in EndoG level, we examined the distribution of cells in the cell cycle. 293T cells were transfected with pS-RT or

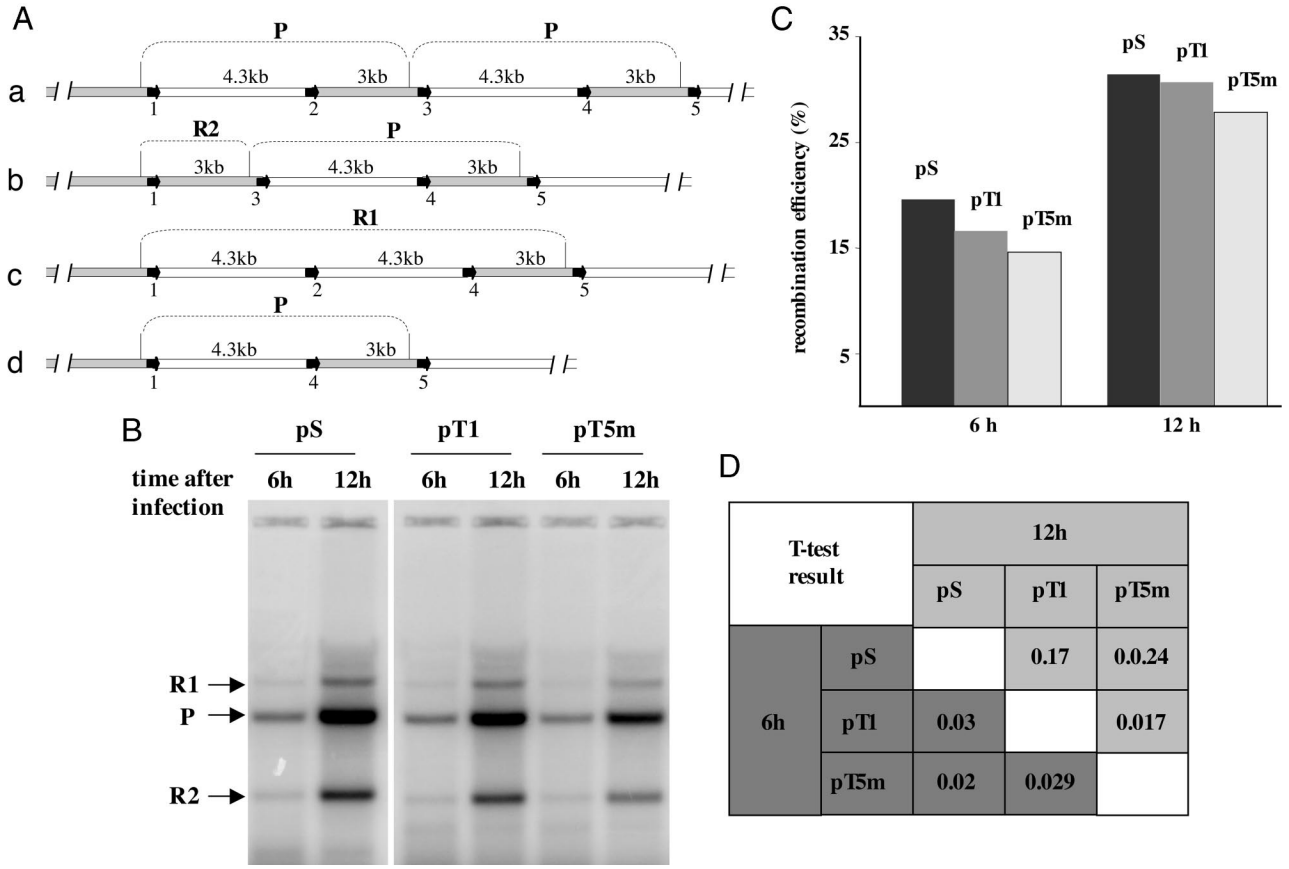

Fig. 3. Analysis of *a* sequence-mediated recombination. (*A*) Illustration of the recombination reaction. (*a*) A pRD105 concatemer showing two units of pRD105 (P). Dark arrows represent HSV-1 *a* sequences in a direct-repeat orientation. The locations of the *a* sequences are indicated as 1–5. NheI cutting sites, a unique site on each pRD105, are indicated as vertical lines. Predicted products (R1 and R2) resulting from recombination reactions between *a* sequence pairs in locations 1 and 2, 2 and 3, and 1 and 3 are indicated in *b*, *c*, and *d* respectively. (*B*) Autoradiogram showing the positions of pRD105 (P) and the recombination products R1 (11.3 kb) and R2 (3 kb). Vero cells were transfected with the indicated plasmids for 5 days and then infected with a mixture of HSV-1 and HSV-1 defective particles containing pRD105 concatemers. After infection for 6 and 12 h, the DNA was extracted and analyzed for pRD105 (P) and the recombination product R2 by Southern blotting followed by hybridization to a ^{32}P-labeled probe, which hybridized to a region in the 3-kb (R2) fragment. (*C*) Summary of recombination products from five experiments as described in *B*. Recombination efficiency is indicated as the R2:P ratio. (*D*) Statistical analysis (*t* test) of differences in recombination efficiency.

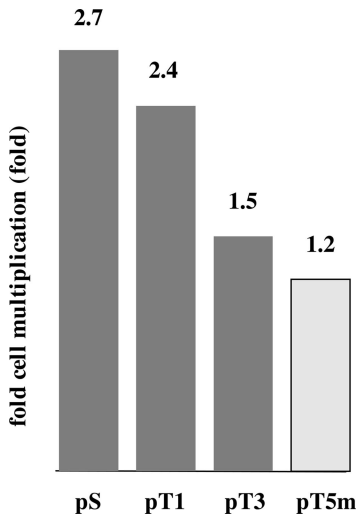

Fig. 4. Effect of reduction of EndoG on cellular proliferation. Growth of cells transfected with pS, pT1, pT3, and pT5m (Fig. 2) was measured in medium containing G418. The -fold increase was determined by comparing the live-cell number when RT-PCR was performed (day 5) with the number of cells seeded 1 day after transfection (day 1). Untransfected cells were undetectable.

pT5m-RT. Twenty-four hours after transfection, the cells were treated with trypsin and seeded onto plates at ≈25% of the original cell density. After the cells were grown in puromycin-containing medium for 2 days, they were stained with propidium iodide (PI), and the distribution of cells in the cell cycle was analyzed by flow cytometry. Fig. 6*A* shows the result of a typical flow cytometry analysis. Fig. 6*B* summarizes the results from three individual experiments. When transfected with pS-RT, 46% of the live cells were in the G_0/G_1 phase, and only 26% were in the G_2/M phase. However, when the cells were transfected with pT5m-RT, the reversal pattern emerged. Only 24% of the live cells were in the G_0/G_1 phase, and 45% were in the G_2/M phase. There was also an increase in cells incorporating less PI, indicative of dead cells with less DNA. Thus, reduction of the level of EndoG changed the cell distribution to a pattern typical of cells arrested at G_2. Furthermore, this G_2 arrest-like pattern could be reversed when pEndoG-GFP was cotransfected with pT5m-RT (data not shown).

Discussion

Our earlier studies demonstrated that uninfected cells could support HSV-1 *a* sequence-mediated recombination that was greatly elevated after HSV-1 infection (14, 15). Because a double-stranded break in DNA is a primary event in the

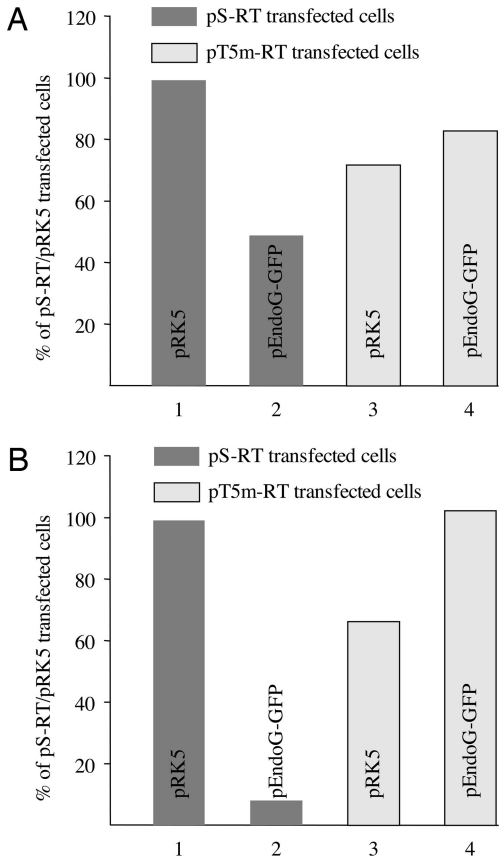

Fig. 5. Rescue of cell-proliferation defect by exogenous expression of EndoG-GFP. (*A*) Summary of live-cell (293T) number relative to that of control cells cotransfected with pS-RT/pRK5 (bar 1), an empty vector that shares a promoter structure similar to that of pEndoG-GFP. Each bar represents cells transfected with 400 ng of each plasmid. Bar 2, cells cotransfected with pS-RT/pEndoG-GFP. Bars 3 and 4, cells cotransfected with pT5m-RT/pRK5 and pT5m-RT/pEndoG-GFP. (*B*) Summary of live-cell (293T) number relative to the control (bar 1). Experiments were performed as described in *A* except 800 ng of each plasmid was used for transfection.

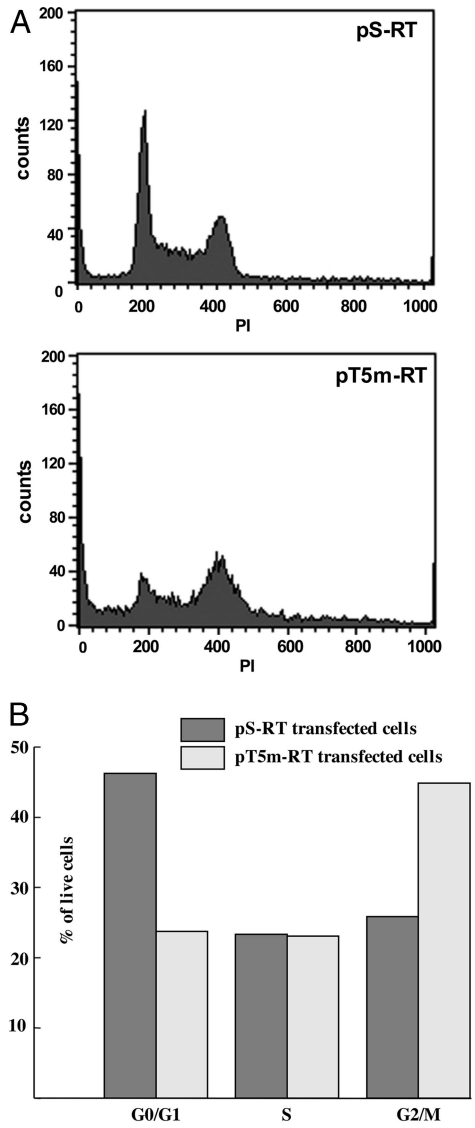

Fig. 6. Distribution of 293T cells transfected with pS-RT and pT5m-RT during the cell cycle. (*A*) FACS histograms show that pS-RT- and pT5m-RT-transfected cells (stained with PI) distribute differently in the cell cycle. (*B*) Summary of cell numbers distributed in the G_0/G_1, S, and G_2/M phases of the cell cycle from three individual experiments as described in *A*.

initiation of recombination, we sought cellular activities that could generate such breaks specifically within the HSV-1 *a* sequence. In a previous study, we purified such an activity from HeLa cells and identified it as a known enzyme, EndoG (6). We further found that EndoG is the only cellular enzyme capable of cleaving the *a* sequence under our experimental conditions. We hypothesized that EndoG initiates both the basal level of recombination in uninfected cells and the elevated level observed during HSV-1 infection. In this study, we sought to assess directly the role of EndoG in the *a* sequence-mediated recombination by using RNA interference to reduce the level of EndoG. We observed a small but statistically significant decrease in *a* sequence-mediated recombination as a consequence of EndoG reduction. There are at least two possibilities to explain the relatively small effect on recombination. (*i*) Although we have reduced the EndoG to a level that causes a cell-proliferation defect, the residual EndoG may be sufficient to initiate a significant level of recombination. (*ii*) EndoG is only one of several enzymes that are capable of initiating recombination at the HSV-1 *a* sequence. At the present time we cannot distinguish between the two possibilities.

In the course of our study we found that cells with a reduced level of EndoG exhibited a proliferation defect. Recent studies with EndoG-deficient mice had shown that, depending on how EndoG was deleted, an EndoG-null mouse could be embryonic-lethal (5) or could show no detectable phenotype (9). The difference appears to originate from the existence of an uncharacterized gene (*D2Wsu81e*) overlapping EndoG in a tail-to-tail orientation on the opposite DNA strand. Like the mouse EndoG gene, the human EndoG gene also overlaps an uncharacterized gene (*C9orf114* or *DKFZp566D143*) in a tail-to-tail orientation on the opposite DNA strand. Although one of our shRNA targets, T5m, is located at a position corresponding to the 3′ untranslated region of *C9orf114*, the cell-proliferation defect that we observe very likely results from a reduction in the EndoG level. Three lines of evidence support this idea. (*i*) No DNA sequence in the sense strand of *C9orf114* bears a significant similarity to that of T5m. In addition, we introduced a mutation in pT5m so that the double-stranded RNA has a mismatch close to the 3′ end of RNA corresponding to the sense strand of EndoG. Such a mutation would be expected to favor RNA-induced silencing complex formation, with the RNA corresponding to the antisense strand of EndoG mRNA and to degrade the

EndoG mRNA instead of *C9orf114* mRNA (19). (*ii*) T1 and T5m (and T3) are at the ends of a 684-bp fragment of EndoG (Fig. 1). Nevertheless, a pattern was observed, in which if a plasmid were to reduce the EndoG level substantially, the cells containing this plasmid would replicate poorly and vice versa. It is therefore difficult to interpret the cell-proliferation defect as an off-target effect. For that to be true, we must assume that the off-target gene contains a sequence and mRNA context very similar to both T1 and T5m; no such gene has been found in GenBank. (*iii*) We were able to express EndoG-GFP and rescue the cell-proliferation defect, indicating that the defect results specifically from the reduced level of EndoG. Our finding of a cell-proliferation defect appears to differ from the results of Irvine *et al.* (9), in which deletion of EndoG failed to produce a detectable phenotype in null mice. Other than the fundamental difference between a tissue culture cell and an intact animal, one possible explanation for the difference is the existence of other enzymes that back up EndoG function. Indeed, we observed that some cells recovering from the growth defect (after 7–9 days of incubation) still had a reduced level of EndoG.

What is the basis of the cell-proliferation defect in cells with reduced levels of EndoG? One hypothesis is that it is because of insufficient EndoG to function in DNA repair, recombination, and/or replication. An earlier study (8) had shown that partially purified bovine EndoG showed a strong affinity for DNA damage caused by L-ascorbic acid, peplomycin, and *cis*-diamminedichloroplatinum(III), suggesting that EndoG can recognize and participate in the repair of local distortions in DNA. Recent studies have also shown that CPS-6, a *Caenorhabditis elegans* homolog of human EndoG, associates directly with *crn*-1, a *C. elegans* homolog of human FEN-1 (20). Human EndoG also forms a complex with FEN-1 (4), a structure-specific endonuclease that removes 5′-overhanging flaps generated during DNA repair, replication, and recombination (21) and that has been shown to play a role in genome stability and mutation sensitivity in yeast and possibly in humans (22, 23). As a binding partner for FEN-1, EndoG could play a similar role. In particular, we have shown that a reduction in EndoG produces a change in cell distribution in the cell cycle that resembles G_2 arrest, one major cause of which is the accumulation of damaged DNA (24).

Materials and Methods

Cell Lines, Bacteria, and Plasmids. African green monkey kidney (Vero) cells were propagated and maintained in DMEM containing 100 units of penicillin G, 100 μg/ml streptomycin, and 292 μg/ml L-glutamine (DMEM-P/S), and 5% FCS. Human embryonic kidney (293T) cells were propagated and maintained in DMEM containing 10% FCS. *Escherichia coli* ECOS 101 competent cells were from Bonature (Westmount, QC, Canada). Plasmid pEndoG-GFP was a gift from Chien-Yun Hsiang (China Medical College, Taiwan).

Construction of Knockdown Plasmids. Knockdown plasmids were constructed based on pS and pS-RT. pS contains nucleotide sequence 1875–7 of pEGFP-N1 (Clontech) and nucleotide sequence 149–995 of p*Silencer* 2.1 neo (Ambion, Austin, TX), with a chloramphenicol-resistance gene inserted between the HindIII site and the BamHI site downstream from the U6 promoter from p*Silencer* 2.1 neo. pS-RT, a derivative of p*Silencer* 5.1 Retro (Ambion), has a chloramphenicol-resistance gene inserted between the HindIII site and the BamHI site of p*Silencer* 5.1-U6 Retro.

To construct the knockdown plasmid, DNA oligonucleotides T1, T3, and T5m, corresponding to EndoG nucleotide sequence 38–56 (T1), 682–700 (T3), and 693–711 with a mutation (A to T) at position 708 (T5m), were designed to transcribe into the stem–loop RNA structure according to instructions from Ambion. The DNA oligonucleotides were chemically synthesized, annealed, and inserted between the BamHI and HindIII sites of pS (or pS-RT), replacing the chloramphenicol-resistance gene. The nucleotide sequences were confirmed by DNA sequencing.

Transfection. Plasmids were delivered into Vero cells with Lipofectamine and the Plus Reagent (Invitrogen) according to the procedure described by Saeki *et al.* (25) with slight modifications. Briefly, a day before transfection, 5–8 $\times$ 10^5 Vero cells were seeded onto a 35-mm plate (or a well in a six-well plate) in DMEM containing 2% FCS. Two micrograms of plasmid DNA was diluted with 125 μl of Opti-MEM (Invitrogen) and mixed with 5 μl of the Lipofectamine Plus reagent for 15 min. Eight microliters of Lipofectamine reagent was diluted with 125 μl of Opti-MEM and mixed with the plasmid DNA–Lipofectamine Plus reagent solution for 30 min. Five hundred microliters of Opti-MEM was added, and the solution was applied to a monolayer of Vero cells that had been washed three times with PBS. After 5 h, the cells were washed once with DMEM containing 6% FCS and incubated with 2 ml of the same medium for overnight growth. Transfection of plasmids into 293T cells was performed with Lipofectamine 2000 (Invitrogen) according to the manufacturer's instructions.

Knockdown of EndoG. For knockdown of EndoG, plasmids pS, pT1, pT3, and pT5m were delivered into Vero cells with Lipofectamine and the Plus Reagent as described above. One day after transfection, the cells were removed from the dish by treatment with trypsin and resuspended in medium (DMEM-P/S/5% FCS) containing 1.5 mg/ml G418 (Geneticin; Invitrogen). The live-cell number was counted, and the cells were distributed into the wells of six-well plates. Approximately 5 days after transfection, the cells were removed from the dish. A portion of the cells was counted with a hemocytometer with 0.2% trypan blue (Invitrogen) to obtain live-cell counts. The remainder of the cells was used for RNA extraction for RT-PCR.

RT-PCR. Total RNA was extracted from cells by using an RNeasy Mini kit (Qiagen, Valencia, CA), and 1 μg of RNA was subjected to reverse transcription by SuperScript III (Invitrogen) according to the manufacturer's instructions. The resulting cDNA was used as the template for the following PCRs: (*i*) the primer pair 5′-GACGACACGTTCTACCTGAGCAAAGTC-3′ and 5′-CCAGGATCAGCACCTTGAAGAAGTG-3′, used to amplify a 241-bp fragment corresponding to nucleotide positions 632–872 of EndoG cDNA; and (*ii*) the primer pair 5′-GGAGTATTCGGGGAAACCTCAAC-3′ and 5′-TGATGCCTACCAACTGTGGGTC-3′, used to amplify a 465-bp fragment corresponding to nucleotide positions 521–985 of hPBGD cDNA. End-point PCRs (denaturation at 94°C for 20 s, hybridization at 65°C for 30 s, and elongation at 72°C for 1 min) were carried out for 35 cycles (for EndoG) or 30 cycles (for hPBGD). The polymerization reactions for the EndoG and hPBGD genes were still in the linear range as determined by quantitative PCR (MJ Research, Cambridge, MA). A mixture of 18 μl of EndoG PCR product and 3 μl of hPBGD PCR product was subsequently analyzed by 2% agarose gel electrophoresis followed by ethidium bromide staining. To determine knockdown efficiency, the intensity of the EndoG band in each lane was normalized to the internal control (hPBGD) band and compared with the normalized EndoG band intensity from the pS-transfected cells. The intensity of each band was quantitated by MAC BASE 1.0 (Fuji).

Preparation of HSV-1 Defective Particles Incorporating Plasmid pRD105. Plasmid pRD105 was incorporated into HSV-1 defective particles according to the procedure described by Yao *et al.* (26) with slight modifications. In brief, pRD105 was delivered into Vero cells with Lipofectamine and the Plus Reagent as described

above. One day after transfection, HSV-1 (Δ305) was used to infect the cells with a multiplicity of infection of ≈20. After a 36-h incubation, 100 μl of the supernatant was used to infect a monolayer of fresh Vero cells on a 60-mm plate with 2 ml of medium. After 36 h, the cells were scrubbed into the medium and subjected to three cycles of freezing and thawing. The clear supernatant obtained from centrifugation at 1,000 × *g* for 10 min was a mixture of HSV-1 defective particles incorporating plasmid pRD105 and active HSV-1 particles.

HSV-1 *a* Sequence-Dependent Recombination Assay. Knockdown of EndoG was as described above. Five days after transfection, the cells in each well of a six-well plate were infected with 50–100 μl of the HSV-1 defective particle mixture plus 2 μl of active HSV-1 (10^9 per ml) in 550 μl of medium (DMEM-P/S/5% FCS) containing 1.5 mg/ml G418. Six and 12 h after infection, the cells were washed twice with PBS and lysed in 500 μl of lysis buffer [50 mM Tris, pH 8.0/2% SDS/10 mM EDTA/4 mM $CaCl_2$/200 μg/ml proteinase K (Roche Molecular Biochemicals)] overnight in a humidified incubator. The total DNA was extracted twice with a phenol/chloroform/isoamyl alcohol (25:24:1) solution (Invitrogen) and precipitated with isopropyl alcohol. The DNA pellets were washed once with 80% (vol/vol) ethanol, dissolved in water, and subjected to restriction enzyme digestion overnight with 30 units of NheI to linearize the amplicon pRD105, and 20 units of DpnI to digest the knockdown plasmids. To remove RNA, 20 μg of RNase A was added in the presence of 50 mM EDTA and incubated at 37°C for 1.5 h. The DNA was extracted twice with the phenol/chloroform/isoamyl alcohol (25:24:1) solution, precipitated with ethanol, and dissolved in TE buffer (10 mM Tris/1 mM EDTA, pH 7.5), and its concentration was measured by spectrophotometry at 260 and 280 nm. To analyze the recombination profile, 7–9 μg of DNA from each sample was separated by 0.8% agarose gel electrophoresis. The DNA fragments were transferred onto a nylon membrane followed by Southern blotting. We labeled the probe, linearized pBluescript (Stratagene), with ^{32}P by using the DECAprime II labeling kit (Ambion) according to the manufacturer's protocol. pRD105 (P) and the recombination product (R2) were quantified with a Typhoon PhosphorImager (Molecular Dynamics) and analyzed by the MAC BAS program.

FACS Analysis. Plasmids pS-RT, pT1-RT, pT3-RT, and pT5m-RT were delivered into 293T cells in a six-well plate by the procedures described above. One day after transfection, cells from each well were removed by treatment with trypsin and resuspended in medium (DMEM/10% FCS) containing 2 μg/ml puromycin (InvivoGENE Biotech, Guangdong, China). Cell numbers were calculated, and cells were appropriately diluted and seeded to dishes so that ≈4 days after transfection, the cell densities of the knockdown plasmid-containing cells were similar (≈60% confluent). The cells were then collected and resuspended in PBS at 1–2 × 10^6 per ml. Cells from 200 μl of the suspension were collected by centrifugation and resuspended in 200 μl of the PI solution [5 μg/ml PI/1 mg/ml RNase A/3% Sopronin (Sigma-Aldrich)/5 mM EDTA in PBS]. After incubation at room temperature for 30 min, the cells were analyzed by FACS sorting.

We greatly appreciate the technical assistance of Bi-Huei Hou with RT-PCR and the *t* test. We also thank Dr. Chien-Yun Hsiang for the kind gift of pEndoG-GFP. This work was supported by National Institutes of Health Grant AI 26538 (to I.R.L.). C.-C.K. was supported by National Institutes of Health Grant AI 20459.

1. Schafer, P., Scholz, S. R., Gimadutdinow, O., Cymerman, I. A., Bujnicki, J. M., Ruiz-Carrillo, A., Pingoud, A. & Meiss, G. (2004) *J. Mol. Biol.* **338,** 217–228.
2. Cote, J. & Ruiz-Carrillo, A. (1993) *Science* **261,** 765–769.
3. Cote, J., Renaud, J. & Ruiz-Carrillo, A. (1989) *J. Biol. Chem.* **264,** 3301–3310.
4. Kalinowska, M., Garncarz, W., Pietrowska, M., Garrard, W. T. & Widlak, P. (2005) *Apoptosis* **10,** 821–830.
5. Zhang, J., Dong, M., Li, L., Fan, Y., Pathre, P., Dong, J., Lou, D., Wells, J. M., Olivares-Villagomez, D., Van Kaer, L., *et al*. (2003) *Proc. Natl. Acad. Sci. USA* **100,** 15782–15787.
6. Huang, K.-J., Zemelman, B. V. & Lehman, I. R. (2002) *J. Biol. Chem.* **277,** 21071–21079.
7. Ohsato, T., Ishihara, N., Muta, T., Umeda, S., Ikeda, S., Mihara, K., Hamasaki, N. & Kang, D. (2002) *Eur. J. Biochem.* **269,** 5765–5770.
8. Ikeda, S. & Ozaki, K. (1997) *Biochem. Biophys. Res. Commun.* **235,** 291–294.
9. Irvine, R. A., Adachi, N., Shibata, D. K., Cassell, G. D., Yu, K., Karanjawala, Z. E., Hsieh, C. L. & Lieber, M. R. (2005) *Mol. Cell. Biol.* **25,** 294–302.
10. Li, L. Y., Luo, X. & Wang, X. (2001) *Nature* **412,** 95–99.
11. Ikeda, S., Hasegawa, H. & Kaminaka, S. (1997) *Acta Med. Okayama* **51,** 55–62.
12. Parrish, J., Li, L., Klotz, K., Ledwich, D., Wang, X. & Xue, D. (2001) *Nature* **412,** 90–94.
13. Roizman, B. & Knipe, D. M. (2001) in *Fields Virology*, eds. Knipe, D. M. & Howley, P. M. (Lippincott Williams & Wilkins, Philadelphia), 4th Ed., Vol. 2, pp. 2399–2459.
14. Dutch, R. E., Bianchi, V. & Lehman, I. R. (1995) *J. Virol.* **69,** 3084–3089.
15. Dutch, R. E., Bruckner, R. C., Mocarski, E. S. & Lehman, I. R. (1992) *J. Virol.* **66,** 277–285.
16. Delius, H. & Clements, J. B. (1976) *J. Gen. Virol.* **33,** 125–133.
17. Hayward, G. S., Jacob, R. J., Wadsworth, S. C. & Roizman, B. (1975) *Proc. Natl. Acad. Sci. USA* **72,** 4243–4247.
18. Umene, K. (1999) *Rev. Med. Virol.* **9,** 171–182.
19. Schwarz, D. S., Hutvagner, G., Du, T., Xu, Z., Aronin, N. & Zamore, P. D. (2003) *Cell* **115,** 199–208.
20. Parrish, J. Z., Yang, C., Shen, B. & Xue, D. (2003) *EMBO J.* **22,** 3451–3460.
21. Harrington, J. J. & Lieber, M. R. (1994) *EMBO J.* **13,** 1235–1246.
22. Tishkoff, D. X., Filosi, N., Gaida, G. M. & Kolodner, R. D. (1997) *Cell* **88,** 253–263.
23. Greene, A. L., Snipe, J. R., Gordenin, D. A. & Resnick, M. A. (1999) *Hum. Mol. Genet.* **8,** 2263–2273.
24. Bunz, F., Dutriaux, A., Lengauer, C., Waldman, T., Zhou, S., Brown, J. P., Sedivy, J. M., Kinzler, K. W. & Vogelstein, B. (1998) *Science* **282,** 1497–1501.
25. Saeki, Y., Breakefield, X. O. & Chiocca, E. A. (2003) *Methods Mol. Med.* **76,** 51–60.
26. Yao, X. D., Matecic, M. & Elias, P. (1997) *J. Virol.* **71,** 6842–6849.